Project - TMA4180 Optimisation 1
Tensegrity Structures

Mari Norfolk
Sebastian Eide Aas
Hans Barstad Westbye
Ola Rønnestad Abrahamsen

March 2024

1 Abstract

This report studies an optimisation model for the problem of form-finding tensegrity structures. We have implemented the BFGS-method with strong Wolfe conditions, a robust algorithm for convex and non-convex unconstrained optimization problems. We will see that in the convex case with only cables in the structure, the algorithm converges quickly regardless of initialisation. When adding bars to the structure, the problem becomes non-convex, but we still obtain a solution reasonably fast using BFGS. We will also see that by the use of a quadratic penalty framework, we manage to solve the constrained optimisation problem easily.

2 Introduction

Tensegrity structures, a synergy of tension and integrity, utilize the equilibrium between compressive forces in rigid bars and tensile forces in flexible cables to maintain stability. Originally artistic concepts, these structures have been adapted for engineering applications, notably in creating adaptive "smart" structures and lightweight designs for space exploration. This project aims to develop an optimization-based model for determining the equilibrium shape of tensegrity structures by analyzing the interplay between their bars and cables.

3 Notation and Definitions

We consider a tensegrity structure modeled as a directed graph $\mathcal{G} = (\mathcal{V}, \mathcal{E})$, where $\mathcal{V} = \{1, \dots, N\}$ denotes the set of nodes representing joints, and $\mathcal{E} \subset \mathcal{V} \times \mathcal{V}$ denotes the set of edges representing bars and cables. The position of a node i is given by $x^{(i)} = (x_1, x_2, x_3) \in \mathbb{R}^3$, with the collective positions of all nodes denoted by $X = (x^{(1)}, \dots, x^{(N)})$. We also denote by e_{ij} with $i < j$ an edge indicating that the joints i and j are connected with a cable or a bar.

3.1 Energy Considerations

The aim is to determine the positions X that minimize the total potential energy of the structure, indicating a stable equilibrium. This involves the consideration of elastic and gravitational energies for both bars and cables, alongside any external loads. We assume that all bars in the structure are made of the same material with the same thickness and cross section, but they may differ in length. The same assumptions are made for cables. We also assume that the weight of the cables are negligible compared to the weight of the bars, that is

$$E_{\text{grav}}^{\text{cable}}(e_{ij}) = 0.$$

For a bar connecting nodes i and j, with resting length ℓ_{ij} and current length $L(e_{ij}) = \|x^{(i)} - x^{(j)}\|$, the elastic energy is modeled as

$$E_{\text{elast}}^{\text{bar}}(e_{ij}) = \frac{c}{2\ell_{ij}^2} \left(L(e_{ij}) - \ell_{ij}\right)^2 = \frac{c}{2\ell_{ij}^2} \left(\|x^{(i)} - x^{(j)}\| - \ell_{ij}\right)^2, \tag{1}$$

where $c > 0$ is a material-dependent parameter. If a bar is either compressed or stretched from the resting length ℓ_{ij} to the new length $L(e_{ij})$, the elastic energy increases. The bar will also experience a gravitational pull which depends on the bar's mass and its z-coordinate. The energy is given by

$$E_{\text{grav}}^{\text{bar}}(e_{ij}) = \frac{\rho g \ell_{ij}}{2} \left(x_3^{(i)} + x_3^{(j)}\right), \tag{2}$$

with ρ being the line density and g the gravitational acceleration.

For cables, the "compression" of the cable does not change its internal energy. The elastic energy for cables is given as

$$E_{\text{elast}}^{\text{cable}}(e_{ij}) = \begin{cases} \frac{k}{2\ell_{ij}^2}\left(\|x^{(i)} - x^{(j)}\| - \ell_{ij}\right)^2, & \text{if} \|x^{(i)} - x^{(j)}\| > \ell_{ij}, \\ 0, & \text{else}, \end{cases} \tag{3}$$

where $k > 0$ is a material constant.

The final energy consideration is the external energy from loads on nodes, which is

$$E_{\text{ext}}(X) = \sum_{i=1}^{N} m_i g x_3^{(i)}, \tag{4}$$

where $m_i \geq 0$ denotes the mass loaded on node i.

Denote by $\mathcal{B}, \mathcal{C} \subset \mathcal{E}$ the bars and cables of the structure, respectively. The total energy of the system is then given by

$$E(X) = \sum_{e_{ij} \in \mathcal{B}} \left(E_{\text{elast}}^{\text{bar}}\ (e_{ij}) + E_{\text{grav}}^{\text{bar}}\ (e_{ij}) \right) + \sum_{e_{ij} \in \mathcal{C}} E_{\text{elast}}^{\text{cable}}\ (e_{ij}) + E_{\text{ext}}(X). \tag{5}$$

3.2 Additional constraints

The first constraint we consider is that some of the positions of some nodes are fixed, that is

$$x^{(i)} = p^{(i)},\ i = 1, ..., M, \tag{6}$$

for a given $p^{(i)} \in \mathbb{R}^3$ and $1 \leq M < N$. This means that we obtain a free optimisation problem. Before solving this problem numerically, we would like to verify that it actually admits a solution.

Claim: The problem of minimising (5) with constraints given by (6) admits a solution, provided that $\mathcal{G}$ is connected.

Proof: To show this, we need to show that (5) is lower semi-continuous and coercive. To show that the function is lower semi-continuous, we will show that it is continuous and then lower semi-continuity will follow.

We see that in equation (5), the only function we must show to be continuous is (3). The reason for this is the fact that both $E_{\text{grav}}^{\text{bar}}$ and E_{ext} are linear polynomials of $x_3^{(i)}$ and $E_{\text{elast}}^{\text{bar}}$ is a quadratic polynomial of X, and thus all three are continuous. Now, let $||x^{(i)} - x^{(j)}|| \to \ell_{ij}$. Then

$$\frac{k}{2\ell_{ij}^2}(||x^{(i)} - x^{(j)}|| - \ell_{ij})^2 \to 0,$$

and therefore (5) is continuous and thus lower semi-continuous.

To show coerciveness, we let at least one $x^{(i)} = p$ be fixed and therefore finite. Further, since $\mathcal{G}$ is connected, there must exist a path from p to all vertices. This implies that at least one edge of the path will tend to ∞ when $\lim_{x \to \infty} ||x - p|| \to \infty$. With this result, we observe that (3) and (1) will tend quadratic to ∞ in terms of the norm. However, there is possibility for a counteracting effect from the gravitational potential from (4) and (2), which will be negative if the x_3 component is negative. Note however, that both of these effects are linear in terms of x_3, and will therefore be dominated by the quadratic effect from (3) and (1). Thus it is coercive, and therefore, the problem of minimising (5) with constraints as in (6) admits a solution. □

The second type of constraint we consider corresponds to a self-supported free-standing structure, with the only constraint is being above ground. This is modeled by

$$x_3^{(i)} \geq f(x_1^{(i)}, x_2^{(i)}),\ i = 1, ..., N, \tag{7}$$

where $f : \mathbb{R}^3 \to \mathbb{R}$ models the height profile of the ground. Similarly as for the last constraint, we would like to verify that we also obtain a solution of (5) with this constraint.

Claim: The problem of minimising (5) with constraints (7) admits a solution if $f \in \mathcal{C}^1(\mathbb{R}^3)$ is coercive.

Proof: Let all masses be positive and non-zero, as a massless structure is not very interesting. Consider a configuration, X, such that the energy in this configuration is $\mathrm{E}(X) := \beta$, and define the lower level set of this energy level, $\mathcal{L}_E(\beta) := \{x \in \mathbb{R}^3 : E(x \leq \beta)\}$. If this set is bounded then the problem $\min_{Y \in \mathcal{L}_E} E(Y)$ has a global solution. Our goal is to demonstrate, by contradiction, that this set is indeed bounded.

Let $\{X_k\} \subset \mathcal{L}_E(\beta)$ be a given sequence of configurations in our level set. Further, we assume the sequence is not bounded and thus we know that $\|X_k\| \to \infty$. However, if $\|X_k\| \to \infty$, then one of the points must tend to infinity. From our constraint $x_3^{(i)} \geq f(x_1^{(i)}, x_2^{(i)})$ we know that if either of the points x_1 or x_2 tends to infinity, then x_3 has to tend to infinity as well. As a consequence of this, the external energy in our system will then tend to infinity, that is

$$\lim_{x_3 \to \infty} E_{\text{ext}}(X) = \lim_{x_3 \to \infty} \sum_{i=1}^{N} m_i g x_3^{(i)} \to \infty.$$

However, this is clearly a contradiction to the fact that $E(X) = \beta$. Our set then has to be bounded, and we thus have a solution. □

In the case of a flat ground profile, $f(x_1, x_2) = 0$, it is not necessarily possible to prove the existence of a solution, as we cannot guarantee coercivity. The reason for this is that the gravitational energy is always zero due to the flat ground profile. Then the only remaining possibility for energy to tend to infinity is for the norm $||x^{(i)} - x^{(j)}||$ to tend to ∞ as discussed in the previous claim. However, this require the constraint of fixing nodes. Therefore, we cannot, without any additional constraints prove the existence of solutions for the case with a flat ground profile.

4 Cable nets

Initially, we will consider a simpler situation, where all egdes in the structure are cables. We have the optimisation problem

$$\min_X E(X) = \sum_{e_{ij} \in \mathcal{E}} E_{\text{elast}}^{\text{cable}}\ (e_{ij}) + E_{\text{ext}}\ (X), \tag{8}$$

with constraints as in (6). We will now study some properties of this objective function.

Claim: The objective function $E(X)$, defined in (8), is $\mathcal{C}^1$ but typically not $\mathcal{C}^2$.

Proof: First, note that the second term in $E(X)$, E_{ext}, is a polynomial of the variable x_3 and is therefore $\mathcal{C}^\infty$. Further $E_{\text{elast}}^{\text{cable}}(e_{ij})$ is also continuous and differentiable for all points except $\|x^{(i)} - x^{(j)}\| = \ell_{ij}$. This leaves to check if the point $\|x^{(i)} - x^{(j)}\| = \ell_{ij}$ is differentiable. First, we note that

$$\lim_{\|x^{(i)} - x^{(j)}\| \to \ell_{ij}^-} \nabla E_{\text{elast}}^{\text{cable}}(e_{ij}) = \nabla 0 = 0.$$

Therefore for the gradient to be continuous, one also need the boundary to go towards 0 from the upper limit. To show this we calculate the partial derivatives:

$$\frac{\partial}{\partial x_1^{(i)}} \frac{k}{2\ell_{ij}^2} \left(\|x^{(i)} - x^{(j)}\| - \ell_{ij} \right)^2 = \frac{k}{\ell_{ij}^2} \left(1 - \frac{\ell_{ij}}{\|x^{(i)} - x^{(j)}\|} \right) (x_1^{(i)} - x_1^{(j)}). \tag{9}$$

This is equivalent for the two other directions. As $\|x^{(i)} - x^{(j)}\| \to \ell_{ij}^+$ the limit goes to 0 and therefore the gradient of $E_{\text{elast}}^{\text{cable}}$ is continuous and $E_{\text{elast}}^{\text{cable}}$ is $\mathcal{C}^1$. The objective function $\mathrm{E}(X)$ is therefore $\mathcal{C}^1$ since it is a sum of $\mathcal{C}^1$ functions.

To check for $\mathcal{C}^2$ continuity we must also calculate the second derivatives. The second derivative will also be equivalent in all directions and it is sufficient to calculate only for one direction. Consider the situations where $\|x^{(i)} - x^{(j)}\| > \ell_{ij}$:

$$\begin{aligned} \frac{\partial}{\partial x_2^{(i)}} \frac{\partial}{\partial x_1^{(i)}} E_{\text{elast}}^{\text{cable}}(e_{ij}) &= \frac{\partial}{\partial x_2^{(i)}} \frac{k}{\ell_{ij}^2} \left(1 - \frac{\ell_{ij}}{\|x^{(i)} - x^{(j)}\|} \right) (x_1^{(i)} - x_1^{(j)}) \\ &= \frac{k}{\ell_{ij}} \frac{(x_1^{(i)} - x_1^{(j)})(x_2^{(i)} - x_2^{(j)})}{\|x^{(i)} - x^{(j)}\|^3}. \end{aligned}$$

Which is not zero as $\|x^{(i)} - x^{(j)}\| \to \ell_{ij}^+$, and therefore not $\mathcal{C}^2$. □

Further, we would like to verify that we actually obtain a solution with our numerical method. Thus we will make use of the following claim:

Claim: The problem (8) is convex, but not strictly convex.

Proof: Given that the sum of convex functions retains convexity, we aim to validate this property for each component of (8). Let us begin with E_{ext}. Recognizing that all linear functions exhibit convexity, but not strict convexity, it follows through linearity of the function that this expression is also convex.

Further since $\mathrm{E}_{\text{elast}}^{\text{cable}}$ is defined piecewise, we can examine each piece. The second piece, $\mathrm{E}_{\text{elast}}^{\text{cable}} = 0$ is convex since it is a constant, but again not strictly convex. Further we know that a norm function is convex and that multiplying with a positive scalar, like $\frac{k}{2\ell_{ij}^2}$, also conserves convexity. Thus, we have left to prove that the expression below is convex,

$$f(g) := \begin{cases} (g - \ell_{ij})^2, & g > \ell_{ij}, \\ 0, & g \leq \ell_{ij}, \end{cases}$$

where $g(x^{(i)}, x^{(j)}) = \|x^{(i)} - x^{(j)}\|$. Differentiating the expression, we obtain

$$f'(g) := \begin{cases} 2(g - \ell_{ij}), & g > \ell_{ij}, \\ 0, & g \leq \ell_{ij}. \end{cases}$$

When $g > \ell_{ij}$, f is a strictly increasing function, and therefore also convex. Combining this, and the fact that multiplying f with a scalar like $\frac{k}{2\ell_{ij}^2}$ conserves convexity, it is clear that $\mathrm{E}_{\text{elast}}^{\text{cable}}$ is also convex. Consequently we can conclude that (8) is convex, but not strictly convex, as neither E_{ext} nor $\mathrm{E}_{\text{elast}}^{\text{cable}}$ is so. □

Since the entire problem (8) is not strictly convex, there is no guarantee that there exists a unique solution. As a consequence of the convexity and differentiability of the function $\mathrm{E}(X)$ in (8), the first order necessary condition is also a sufficient condition. Therefore, X^* is global minimiser if and only if

$$\nabla \mathrm{E}(X^*) = 0, \tag{10}$$

which is the necessary and sufficient conditions for (8).

5 Tensegrity-domes

In this case, we want to consider a situation were we have both bars and cables in the structure, but still with constraint of fixed nodes as in (6). These structures are sometimes called tensegrity-domes. The optimisation problem we obtain is

$$\min_X E(X) = \sum_{e_{ij}\in\mathcal{B}} (E^{\text{bar}}_{\text{elast}}(e_{ij}) + E^{\text{bar}}_{\text{grav}}(e_{ij})) + \sum_{e_{ij}\in\mathcal{C}} E^{\text{cable}}_{\text{elast}}(e_{ij}) + E_{\text{ext}}(X). \tag{11}$$

Because of the interaction between the tension in the cables and the stresses in the bars, we can now obtain structures that rise above the ground. To obtain such a result numerically, we first need some theoretical background.

Claim: The optimisation problem (11) is non-convex if $\mathcal{B} \neq \emptyset$.

Proof: First, define

$$f(\cdot) = \sum_{e_{ij}\in\mathcal{B}} \frac{c}{2\ell_{ij}} (|| \cdot^i - \cdot^j || - \ell_{ij})^2.$$

Assume that $\lambda = \frac{2}{3}$ and that X and Y is such that

$$||x^{(i)} - x^{(j)}|| = 3||y^{(i)} - y^{(j)}|| = \ell_{ij}.$$

Further, $X = -3Y$ such that

$$f(\lambda X + (1-\lambda)Y) = f(\frac{2}{3}X + \frac{1}{3}Y) = f(\frac{2}{3}X - \frac{2}{3}X) = f(0) = \sum_{e_{ij}\in\mathcal{B}} \frac{c}{2\ell_{ij}^2}(||0|| - \ell_{ij})^2 = \sum_{e_{ij}\in\mathcal{B}} \frac{c}{2}.$$

However, as a result of our assumptions for X and Y we also obtain

$$\begin{aligned} f(\lambda X + (1-\lambda)Y) = f(\frac{2}{3}X + \frac{1}{3}Y) &\leq \frac{2}{3}f(X) + \frac{1}{3}f(Y) \\ &= \sum_{e_{ij}\in\mathcal{B}} \Big[\frac{c}{3\ell_{ij}^2}(||x^{(i)} - x^{(j)}|| - \ell_{ij})^2 + \frac{c}{6\ell_{ij}^2}(||y^{(i)} - y^{(j)}|| - \ell_{ij}^2)^2\Big] \\ &= \sum_{e_{ij}\in\mathcal{B}} \Big[\frac{c}{3\ell_{ij}^2}(\ell_{ij} - \ell_{ij})^2 + \frac{c}{6\ell_{ij}^2}(\frac{1}{3}\ell_{ij} - \ell_{ij})^2\Big] = \sum_{e_{ij}\in\mathcal{B}} \frac{2c}{27}. \end{aligned}$$

And thus the following requirement for convexity with $\lambda = \frac{2}{3}$ does not hold:

$$f(\lambda X + (1-\lambda)Y) = \sum_{e_{ij}\in\mathcal{B}} \frac{c}{2} \not\leq \sum_{e_{ij}\in\mathcal{B}} \frac{2c}{27} = \lambda f(X) + (1-\lambda)f(Y).$$

Thus the entire problem (11) is non-convex if $\mathcal{B} \neq \emptyset$. □

The objective function in (11) is usually not differentiable. To see this, we look at (9), as this is the general derivative for the case with a bar. Because of the division with the norm, the objective function can not deal with points being close with eachother, as we will divide by 0. This typically imposes a numerical problem, but in practical situations, this problem does not occur. The reason for this is that the bars typically will not have a length that is close to 0.

Because our problem is neither convex nor differentiable, we can not expect our numerical method to converge to a global minimiser. However, we can still obtain local minimisers. We still have the same optimality conditions, that is

$$\nabla E(X^*) = 0, \tag{12}$$

but since the problem is non-convex for $\mathcal{B} \neq \emptyset$, the conditions are not sufficient for a global minimum. However, we are more interested in local minimums as our goal is to achieve a stable system given our initialisation. From Figure 1 we observe how different local minimums are found dependent on the initialisation, which shows that (11) may admit non-global minimisers.

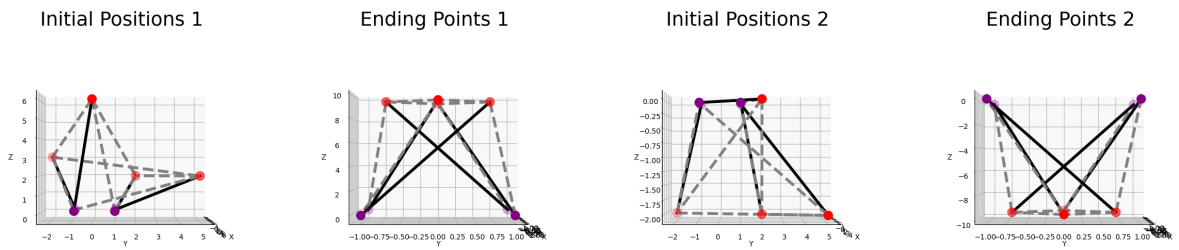

Figure 1: Numerical solution of (11) with constraints as in (6). Red points are the free nodes, while purple are fixed. The dotted lines indicate cables between the nodes, while the solid lines indicate bars.

6 Free-standing structures

In this case, the only constraint we have is that the structure remains over ground such that we obtain a free-standing structure. This leads to the optimisation problem

$$\min_X E(X) = \sum_{e_{ij}\in\mathcal{B}} (E^{\text{bar}}_{\text{elast}}(e_{ij}) + E^{\text{bar}}_{\text{grav}}(e_{ij})) + \sum_{e_{ij}\in\mathcal{C}} E^{\text{cable}}_{\text{elast}}(e_{ij}) + E_{\text{ext}}(X), \tag{13}$$

with constraints as in (7).

Note that there are no equality constraints present. Thus, the first order optimality conditions for (13) reads

$$\begin{aligned} \nabla E(X^*) &= \sum_{i\in\mathcal{I}} \lambda_i^* \nabla c_i(X), \\ x_3^{(i)} &\geq f(x_1^{(i)}, x_2^{(i)}), \\ \lambda_i^* &\geq 0 \ \forall \ i \in \mathcal{I}. \end{aligned}$$

The linear constraint qualifications (LICQ) holds if the vectors

$$\nabla c_i(X) \ \forall \ i \in \mathcal{A}(X),$$

where $\mathcal{A}(X) \subset \mathcal{I}$, are linearly independent. In our case, every vector will have the non-zero element in different places as we always use the third element in each point for different values of $i \in \mathcal{A}(X)$. Thus LICQ holds and the KKT-conditions are necessary for a local solution. However, they are not sufficient, as we showed that the objective function in (11) is non-convex for $\mathcal{B} \neq \emptyset$.

7 Numerical methods

For every optimisation problem discussed so far, we have chosen to implement the BFGS-method described in Algorithm 6.1 in [NW06] with strong Wolfe conditions. The reason for the choice of a Quasi-Newton method is the superlinear rate of convergence. In addition, it does not require a positive definite Hessian, which is convenient in our case as we do not have an objective function which is typically twice continuously differentiable.

We initialised the linesearch inspired by Algorithm 3.5 in [NW06] with $c_1 = 10^{-4}$ and $c_2 = 0.9$, which are commonly used values for this kind of implementation. Initialising the step length $\alpha = 1$ leads to faster computations as we often take a good step in the first iteration. When finding an approximate Hessian in BFGS, it is important to implement it with caution to avoid unnecessary computations. The Hessian was computed as

$$H_{k+1} = H_k - \rho_k(s_k \otimes (H_k y_k) + (H_k y_k) \otimes s_k) + \rho_k(1 + \rho_k \langle y_k, H_k y_k \rangle) s_k \otimes s_k,$$

where $\otimes$ represents the outer product. The first Hessian is initialised as the identity matrix.

We have used the quadratic penalty framework with BFGS from [NW06] to solve the constrained optimisation problem. The penalty function is defined as

$$Q(X, \mu) := E(X) + \frac{\mu}{2} \sum_{i \in \mathcal{I}} c_i^-(X)^2,$$

where $c_i^-(X) = \max\{-c_i(X), 0\}$ and $c_i(X)$ is the constraint as in (7). The convergence criteria we have set is

$$\sum_{i \in \mathcal{I}} c_i(X)^2 < \text{tol},$$

where tol is some set tolerance which needs to be modified to give good solutions for different initial setups.

8 Results and discussion

Having established the necessary theory and numerical methods, we proceed to analyze the various cases numerically.

8.1 Cable nets

We first want to solve (8) with constraints as in (6), i.e. a structure with only cables. We have used four fixed nodes for our test case, denoted as $p^{(i)}$ for $i = 1, 2, 3, 4$, and four free nodes $x^{(j)}$ for $j = 5, 6, 7, 8$. In addition, we have used the parameters

- $k = 3$,
- $\ell_{ij} = 3$ for all edges (i, j),
- $p^{(1)} = (5, 5, 0), p^{(2)} = (-5, 5, 0), p^{(3)} = (-5, -5, 0), p^{(4)} = (5, -5, 0)$,
- $m_i g = \frac{1}{6}$ for $i = 5, 6, 7, 8$.

The analytical solution is given as

Table 1: Analytical and numerical solutions of (8).

Node	Initial	Analytical	Numerical
$x^{(5)}$	$(3, 5, -4)$	$(2, 2, -\frac{3}{2})$	$(2, 2, -\frac{3}{2})$
$x^{(6)}$	$(-3, 4, -2)$	$(-2, 2, -\frac{3}{2})$	$(-2, 2, -\frac{3}{2})$
$x^{(7)}$	$(-3, -5, 0)$	$(-2, -2, -\frac{3}{2})$	$(-2, -2, -\frac{3}{2})$
$x^{(8)}$	$(3, -5, -4)$	$(2, -2, -\frac{3}{2})$	$(2, -2, -\frac{3}{2})$

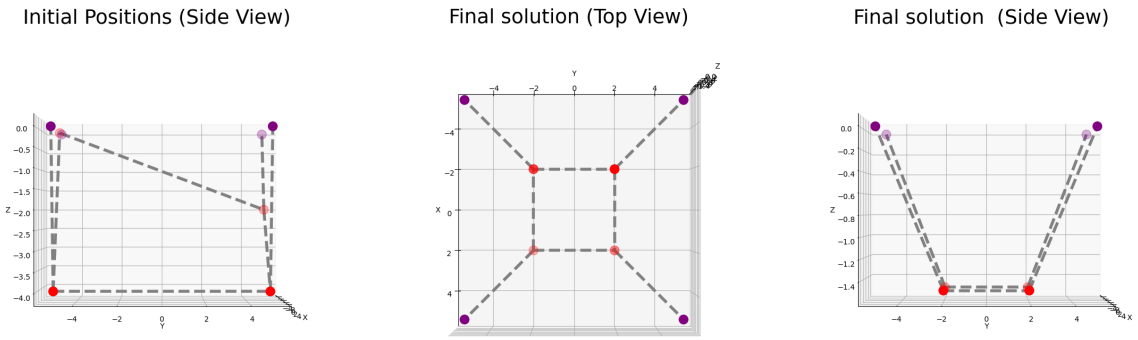

Figure 2: Numerical solution of (8) with constraints as in (6). Red points are the free nodes, while purple points are fixed. The dotted lines indicate cables between the nodes.

As we can see from Figure 2, our numerical solution coincides well with the analytical solution. Our method used 57 iterations and we were able to verify that our optimality conditions in (10) was satisfied up to machine precision. As mentioned in Section 4, this is a unique, global minimiser and it is independent of initialisation. This is verified by Figure 3. In this plot, we set the free points randomly but keep the rest of the parameters equal to above, and the method used 67 iterations to reach the global solution. The result also makes sense physically, because of the gravitational pull of the free nodes by equation (4). Since we do not have any constraint that ensures the structure to remain above ground, this is an expected result.

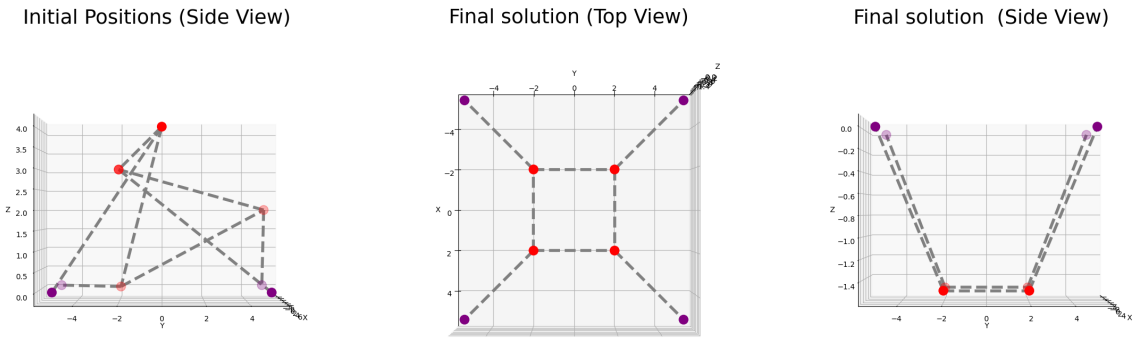

Figure 3: Numerical solution of (8) with constraints as in (6) and random initialisation of free points. Red points are the free nodes, while purple points are fixed. The dotted lines indicate cables between the nodes.

8.2 Tensegrity-domes

Further we want to solve (11) with constraints as in (6), which is a tensegrity structure with cables and bars. We have used a test case with four fixed nodes $p^{(i)}$ for $i = 1, 2, 3, 4$ and four free nodes, $x^{(j)}$ for $j = 5, 6, 7, 8$, and used the parameters

- $\ell_{15} = \ell_{26} = \ell_{37} = \ell_{48} = 10$,
- $\ell_{18} = \ell_{25} = \ell_{36} = \ell_{47} = 8$,
- $\ell_{56} = \ell_{67} = \ell_{78} = \ell_{58} = 1$,
- $c = 1$, $k = 0.1$, $g\rho = 0$,
- $p^{(1)} = (1, 1, 0), p^{(2)} = (-1, 1, 0), p^{(3)} = (-1, -1, 0), p^{(4)} = (1, -1, 0)$,
- $m_i g = 0$ for $i = 5, 6, 7, 8$.

The analytical solution of this problem is given in Table 2 below.

Table 2: Analytical and numerical solutions of (11), with $s \approx 0.70970$ and $t = 9.54287$.

Node	Initial	Analytical	Numerical
$x^{(5)}$	$(3, 2, 2)$	$(-s, 0, t)$	$(-0.70971, 0, 9.54287)$
$x^{(6)}$	$(4, 5, 2)$	$(0, -s, t)$	$(0, -0.70971, 9.54287)$
$x^{(7)}$	$(2, -2, 3)$	$(s, 0, t)$	$(0.70971, 0, 9.54287)$
$x^{(8)}$	$(6, 0, 6)$	$(0, s, t)$	$(0, 0.70971, 9.54287)$

Recall from Section 5 that the objective function in (11) is non-convex as we include bars in this problem. Therefore, there exists other solutions to the problem as well and we might obtain a different result with respect to the initialisation.

We observe from Figure 4 that we converge to the analytical solution given in Table 2 above, and again we are able to confirm that the optimality conditions given in (12) are satisfied up to machine precision. In this case, we used 191 iterations. This is reasonable as the problem is non-convex and we may need more iterations to converge to a stable solution. We observe that the bars have the same length as they are initialised, while the cables are stretched. A difference between this structure and the one in Figure 2, is that this structure remains over ground. As discussed earlier, this is due to the interaction between the tension in the cables and the stresses in the bars.

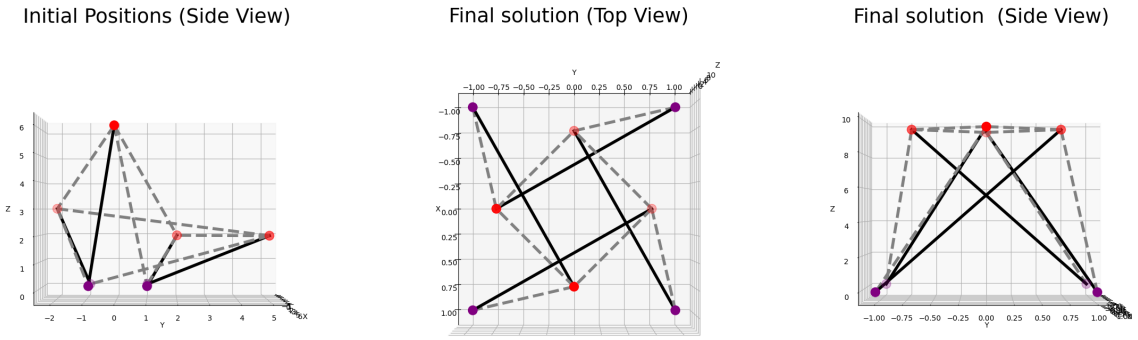

Figure 4: Numerical solution of (11) with constraints as in (6). Red points are the free nodes, while purple points are fixed. The dotted lines indicate cables between the nodes, while the solid lines indicate bars.

8.3 Free-standing structures

The last case we want to investigate is the case of a free-standing tensegrity structure. We are thus solving (11) with constraints as in (6). We have used the parameters from the last case with the additional cables lengths set to 2, the parameter $\rho g = 10^{-4}$ and the height profile

$$f(x_1, x_2) = \frac{x_1^2 + x_2^2}{20}.$$

This setup results in a solution that is close to the optimum in the previous case. The gradient of the quadratic penalty function is then approximately 0, verifying the accuracy of our code. We see from Figure 5 that the solution resembles Figure 4. Since we also can have local solutions in this case, the final solution will be strongly influenced by the initial positions. Therefore, we had to initialise the starting positions close to the optimum in the previous case, though with free nodes. The bars are slightly compressed in this case, while the cables have been stretched.

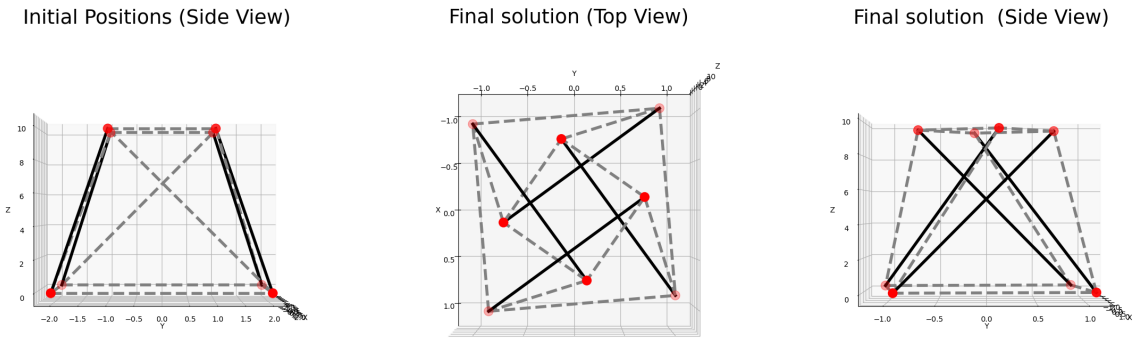

Figure 5: Numerical solution of (13) with constraints as in (7). Red points are the free nodes. The dotted lines indicate cables between the nodes, while the solid lines indicate bars.

We have also stacked two structures on top of each other with same setup as above, but with $mg = 10^{-2}$ and $\rho g = 10^{-4}$. This is shown in Figure 6, and we see that also with mass on the nodes, the structure rises above ground in this case as well. The structure seems physically reasonable, and the gradient is approximately zero, which further verifies our numerical implementation.

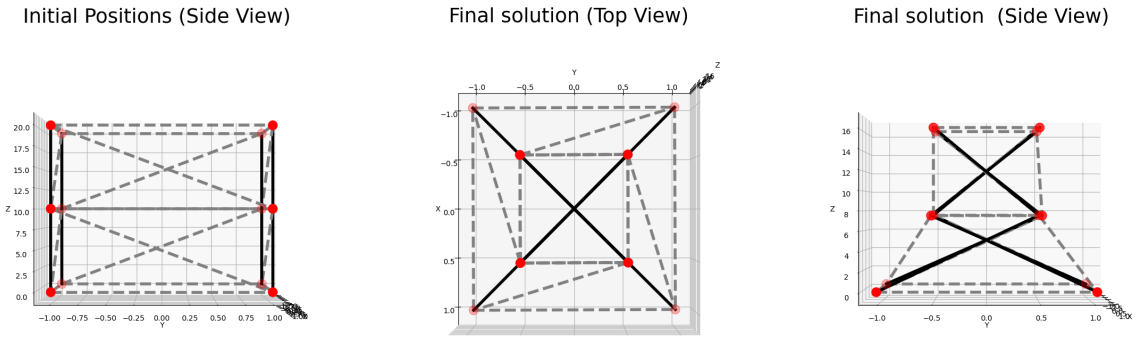

Figure 6: Numerical solution of (13) with constraints as in (7). Red points are the free nodes. The dotted lines indicate cables between the nodes, while the solid lines indicate bars.

9 Conclusion

We can conclude that the BFGS method with strong Wolfe conditions worked very well on the convex and non-convex unconstrained optimisation problems. In the case of only cables in the tensegrity structures and the constraint of fixed nodes, we obtained a unique global solution which coincides with the theoretical results. When adding bars to the structure and keeping the fixed nodes, we observed that we get a reasonable numerical result despite the non-convexity of the problem. In the constrained scenario, we similarly achieved a numerically reasonable outcome, though the method displayed greater sensitivity to initial conditions and parameter selection to obtain physically feasible solutions.

References

[NW06] Jorge Nocedal and Stephen J. Wright. *Numerical Optimization*. 2e. New York, NY, USA: Springer, 2006.